Provisional chapter

Noninvasive Monitoring of Manual Ventilation during Out-of-Hospital Cardiopulmonary Resuscitation

Andoni Elola, Erik Alonso, Elisabete Aramendi and Unai Irusta

Additional information is available at the end of the chapter

Abstract

Cardiopulmonary resuscitation (CPR) consisting of chest compressions and assisted ventilation is crucial to treat out-of-hospital cardiac arrest (OHCA). It is well reported that quality of manual ventilations, in terms of rate and volume, is suboptimal, with a high incidence of hyperventilation, which is linked to poor outcomes. The lack of a noninvasive technology to monitor ventilations during out-of-hospital CPR precludes feedback on ventilations to the rescuer, and it handicaps the evaluation of the effect of ventilations on the outcome of the patient. This chapter addresses the possibilities and challenges of monitoring the quality of manual ventilations in current defibrillators. Methods are proposed to monitor ventilations based on the thoracic impedance and the capnogram. These methods can be integrated in defibrillators used in both basic and advanced life support. The algorithms are described, and the accuracy of the methods to monitor the ventilation rate and the quality metrics of the ventilations is reported using real OHCA episodes. The accuracy and limitations of the methods as well as the implications of integrating them in the treatment of patients in cardiac arrest are discussed.

Keywords: manual ventilation, cardiopulmonary resuscitation, out-of-hospital cardiac arrest, thoracic impedance, capnogram

1. Introduction

Sudden cardiac arrest is the sudden cessation of effective blood circulation due to heart failure. If not treated promptly, cardiac arrest can lead to sudden cardiac death within minutes [1]. Sudden cardiac death is one of the leading causes of death in the industrialized world [2, 3].

Although the overall incidence depends on the definition and inclusion criteria applied by each study, it is documented that it ranges from 150,000 to 530,000 person-year in the United States, and about 275,000 in Europe [1, 2, 4].

Most cardiac arrest occur in the out-of-hospital setting [5]. There are two levels of treatment for out-of-hospital cardiac arrest (OHCA), basic life support delivered by emergency medical technicians and advanced life support (ALS) with the intervention of clinicians. Despite important progress in epidemiology, profiling and treatment of OHCA in the last decades, the survival rates to hospital discharge are dismally low, with rates between 8.4 and 10.7% [2, 6].

In OHCA, the first minutes are crucial as the chances of the patient to survive decrease about 10% per minute [7]. The chain of survival defines the key steps to treat a person in cardiac arrest. Two of the most important links of the chain are early defibrillation and early cardiopulmonary resuscitation (CPR). Defibrillation is delivered either by an automated external defibrillator (AED) or by more advanced monitor defibrillators used by ALS clinicians. The objective of CPR is to maintain a minimum oxygenated blood flow to the heart and brain until advanced care is available.

Quality of CPR is a key factor for the survival of OHCA patients. The 2015 resuscitation guidelines recommend that chest compression are provided with a rate of at least 100 compressions per minute and a depth of 5 cm [8]. During CPR, two ventilations may be given between series of chest compressions before intubation. Lay rescuers should open the airway using a head-tilt-chin-lift maneuver and blow steadily into the mouth while watching for the chest to rise, as shown in **Figure 1** [9]. The time taken to give a ventilation should be around 1 s, with no more than 5 s for two ventilations. After intubation, the resuscitation guidelines recommend CPR including continuous bag-mask ventilation with and without supplementary oxygen, as shown in **Figure 2**. The recommended ventilation rate is about 1 breath every 5–6 s, or about 10–12 breaths per minute [11]. However excessive ventilation, either by rate or tidal volume is

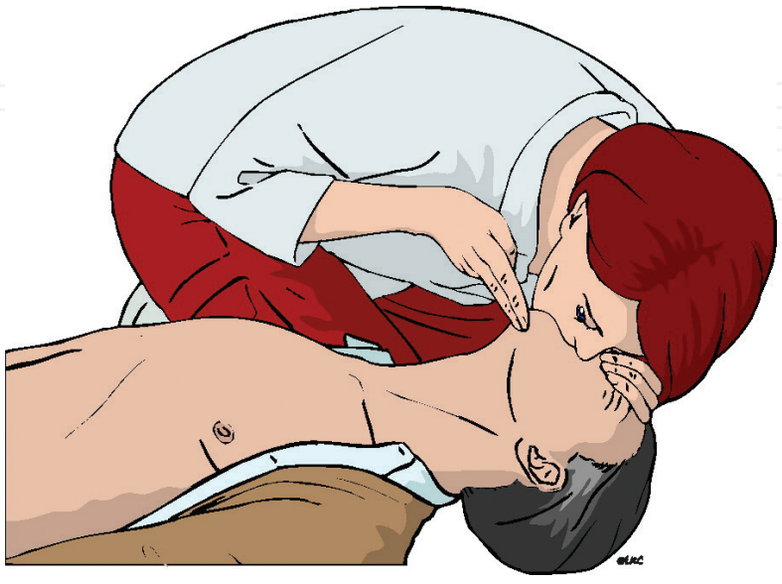

Figure 1. Head-tilt-chin-lift maneuver to provide ventilations. Extracted from [9].

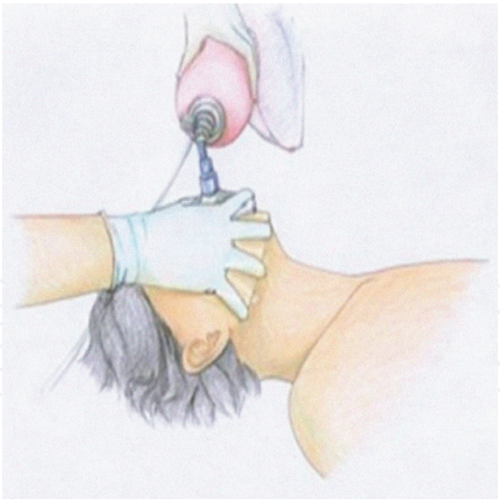

Figure 2. Bag-mask ventilation. Extracted from [10].

common during resuscitation [12–16]. Several analyses on OHCA episodes report rates ranging from moderate (14 min^{-1}) to severe (>20 min^{-1}) hyperventilation.

The negative effect of hyperventilation during CPR is well known: it increases intrathoracic pressures, reshapes the oxygen dissociation curve (increasing oxygen affinity) and behaves as a cerebral vasoconstrictor [17, 18]. Many studies have also proven that it contributes to a lower coronary perfusion pressure and to hemodynamic deterioration in animals [19, 20]. All these factors decrease the probability of survival of a patient in cardiac arrest, so the monitoring and evaluation of ventilation during CPR.

The real-time monitoring of the instantaneous ventilation rate during OHCA would enable feedback to the rescuers, so they could adhere to current guidelines. Furthermore, retrospective evaluation of the ventilation rates may help in debriefing to improve the quality of CPR provided by emergency medical services. Unfortunately, no commercial systems are available for BLS or ALS defibrillation equipment that give real-time feedback to the providers, and no automatic methods are available for debriefing on the quality of ventilation. Several quality metrics have been proposed to monitor quality of ventilations in OHCA [21], such as the mean value of ventilations delivered per minute and the fraction of minutes with hyperventilation (FMH), that is ventilation rates above 15 min^{-1}.

The automated computation of those ventilation quality values requires ventilation detection algorithms based on signal processing of the biomedical signals recorded by commercial equipment. Nowadays, equipment to monitor gas exchange during ventilations is not routinely used in OHCA, in contrast to the ubiquitous mechanical ventilators used in-hospital. In the BLS scenario, the biomedical signals recorded by AEDs through the defibrillation pads (see **Figure 3**) are most frequently the electrocardiogram (ECG) and the thoracic impedance (TI). Ventilations are visible in the TI as fluctuations in the waveform with every insufflation of oxygen into the chest of the patient. For more advanced monitor-defibrillators, as the ones used by medical experts in ALS, additional modules like the capnogram are available. Capnography monitors the partial pressure of the CO_2 in the respiratory gasses, and reflects high concentration during the exhalation phase of every ventilation.

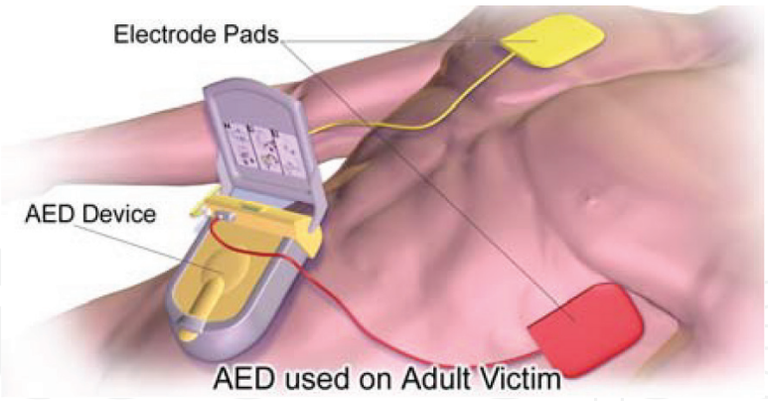

Figure 3. Automated external defibrillator with electrode pads attached to a patient. Source: BruceBlaus, CC BY-SA 4.0 https://creativecommons.org/licenses/by-sa/4.0, via Wikimedia Commons.

In this chapter, the feasibility of monitoring the ventilation rate is analyzed using first the TI and then the capnogram. Automatic methods to detect ventilations are described, and their accuracy reported with OHCA datasets. The performance of the algorithms is reported in terms of sensitivity (SE), the percentage of correctly detected ventilations, and positive predictive value (PPV), the percentage of detected ventilations that are true ventilations. The validity of those methods to monitor the instantaneous ventilation rate and to evaluate the quality of ventilation is also analyzed. Finally, this chapter concludes with a discussion of several key points to be considered before these methods could be integrated into commercial equipment.

2. Thoracic impedance for ventilation monitoring

The TI is measured though the defibrillation pads of a defibrillator attached to the chest of the patient in the anterolateral position, as shown in **Figure 3**. A high frequency excitation current (20–100 kHz at 1–5 mA) is applied through the pads and the resulting surface potential measured to compute the impedance by applying Ohm's law. The TI may show different components:

- *Baseline component*: a baseline impedance value of 50–120 Ω depending on the position of the pads and on the patient's sex, chest size and body mass [22].
- *Chest compression component*: chest compressions cause variations in the cross-sectional area of the chest [23] and mechanical disturbances in the defibrillation pads that are reflected in the TI as fluctuations of amplitudes between 0.15 Ω and several ohms [24, 25].
- *Ventilation component*: ventilations produce variations in the cross-sectional area of the thorax [23]. Inflation of the lungs causes an increase in impedance because air is a poor conductor of electric current [25]. The TI shows a fluctuation from 0.1 Ω to 8 Ω with each ventilation [26, 27].
- *Circulation component*: the impedance shows a small fluctuation (<100 mΩ) with each effective heartbeat [26, 28, 29].
- *Additional noise and artifacts*: other noise and artifacts due to movement, electrode-skin contact, and so on can be present in the impedance [30].

All these components can be observed in **Figure 4**. From top to bottom, the ECG, TI, the compression depth (CD) of the chest compressions and the capnography are depicted. The TI shows a baseline around 105 Ω and fluctuations due to chest compressions (around 1 Ω), ventilations (0.5–1 Ω), and circulation (0.1 Ω). There is a perfect match between (1) compressions in the CD signal and fluctuations due to compressions in the TI signal, (2) the capnogram and fluctuations due to ventilations in the TI, and (3) effective heartbeats in the ECG and the circulation component in the TI. Two ventilations are visible in the TI, the fluctuations around 14 and 18 s, which correlate with increases of the CO_2 expired in the capnogram.

The TI has become a very useful signal in an OHCA in the last two decades and it is recorded by every commercial defibrillator, either AED or monitor/defibrillator. In 2002, Pellis et al. first suggested that ventilations (respirations) cause measurable fluctuations in the TI signal [27]. In an experiment with anesthetized male pigs, they found out that TI measurement at frequencies between 0.1 and 2 Hz showed fluctuations that were time coincident with the ventilations in the capnography signal.

Later in 2006, Losert et al. analyzed the feasibility of monitoring the ventilation characteristics during CPR using the TI signal acquired by the defibrillation pads of an AED [26]. They analyzed the correlation between the amplitude of the TI fluctuation due to ventilation and the tidal volume (400–1000 mL) given by a ventilator. They concluded that the TI

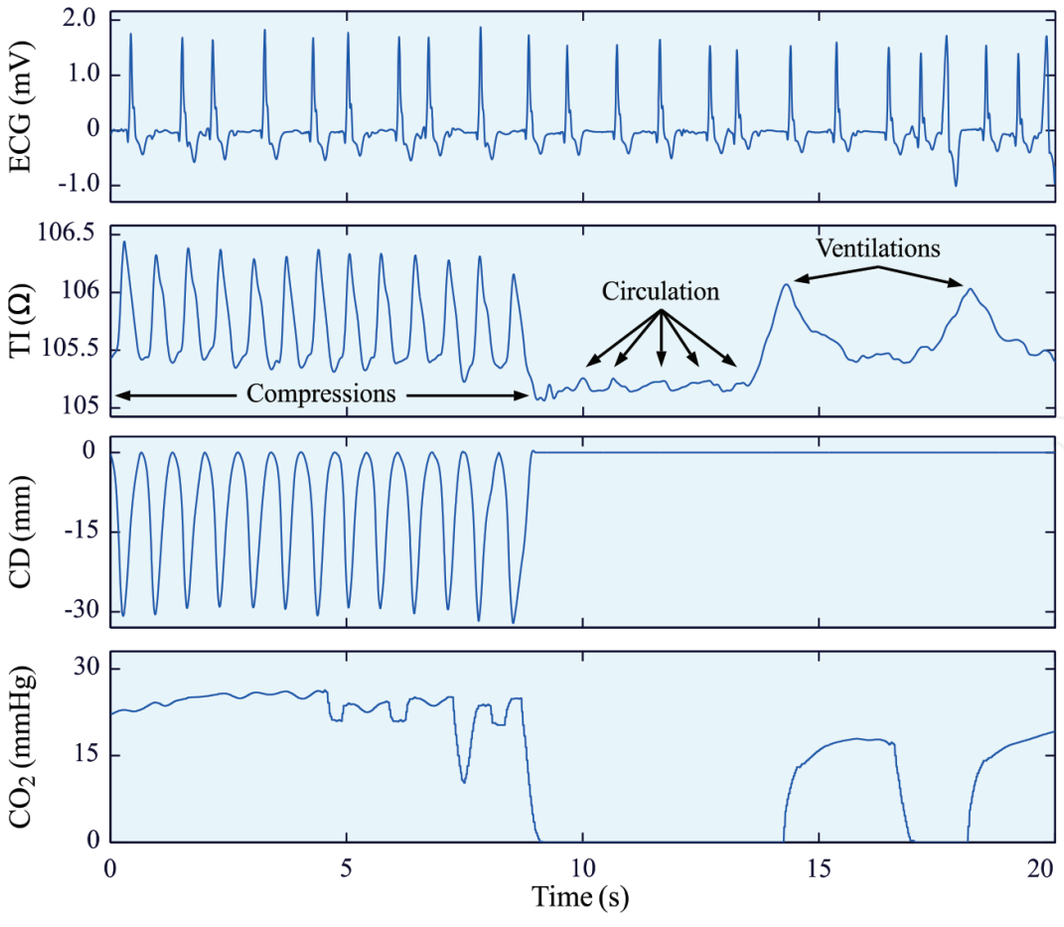

Figure 4. From top to bottom, the ECG, TI, CD and capnography signals are represented. Two ventilations are visible in the TI around 14 and 18 s.

allows to compute ventilation rates, inspiration and expiration times, but the amplitude of the TI fluctuation was not valid for exact tidal volume estimation. More recently, Roberts et al. also investigated the relationship between tidal volume and TI amplitude fluctuations but in mechanically ventilated children and using the TI acquired for two different placements of the defibrillation pads, anterior-apical and anterior-posterior positions [31]. The ventilations in the TI were detected as fluctuations above 0.4 Ω. The study concluded that although the linearity between tidal volume and TI fluctuation was high for each individual, it was not feasible to derive the exact tidal volume from the TI fluctuation for the pediatric population as a whole. The study also showed that the TI acquired via defibrillation pads could be used to accurately detect ventilations if delivered according to the guidelines (7–10 ml/kg tidal volume), with no significant differences between pad positions for ventilation detection. Nevertheless, for smaller volumes (<7 ml/kg), the sensitivity for ventilation detection decreased, suggesting that shallow ventilations during CPR might not be detected in the TI.

These evidences motivated Risdal et al. to propose a ventilation detector during CPR based on the TI signal [32]. After a preprocessing stage, the fluctuations in the TI due to chest compressions were suppressed using an adaptive filtering scheme [33]. The ventilation detector was based on a neural network classifier. The classifier decided whether each TI segment (1.4 s) analyzed was an expiration onset (maximum peak of the fluctuation in the TI) in the basis of waveform features extracted from the analyzed segment. This was a novel and complex approach to detect ventilations with excellent performance (SE/PPV of 90.4%/95.5%). However, ventilations were manually annotated in the TI signal and used as gold standard to evaluate the performance of the ventilation detector. Therefore, still there was the need for a more reliable validation using a robust independent gold standard. Furthermore, the complexity and computational burden of the method limited its application.

More recently, Edelson et al. developed two different ventilation detection algorithms, one based on the TI and other based on the capnography signal [34]. They hypothesized that capnography would be superior to TI for measuring ventilation rate, and that a combined algorithm would be more accurate than one based on a single signal. They obtained slightly better results in terms of SE/PPV for the capnography-based detector: 78%/87% for the TI-based detector, and 82%/91% for the capnography-based detector. As hypothesized the combination of both algorithms showed better performance. The lack of a gold standard (spirometry, flow or volume of the ventilations) independent of the signals used to develop the detectors might have affected the results.

2.1. An automated ventilation detector based on the TI

In this section, we present a study carried out to overcome the main limitations of the works described earlier and to cast some light on the reliability and accuracy of the TI to compute ventilation metrics. The study is aimed at (1) developing a simple ventilation detector based on the TI that might be incorporated into current commercial defibrillators; and (2) computing the CPR quality metrics related to ventilations in order to evaluate their accuracy against a robust gold standard.

The dataset used to carry out the study consisted of OHCA episodes recorded through the Philips MRx monitor/defibrillator between 2006 and 2009 by the Tualatin Valley Fire and Rescue in Portland, OR, USA. Each episode contained concurrent TI and capnography signals for at least 30 min. The capnogram was considered the gold standard for the instants of ventilations which were manually and independently annotated by three experienced biomedical engineers. Intervals where the ventilation pattern was not clearly recognizable were excluded from the analysis. A total of 2575 min were analyzed, which included 17,586 ventilations. Episodes were randomly allocated to training and test sets, 32 and 31 episodes respectively. **Figure 5** shows an epoch of an episode included in the dataset of the study where capnography and TI signals are depicted, and the instants of ventilations are marked as black dotted lines on the capnogram.

The ventilation detector was developed using the training set and consisted of three different stages. First, a preprocessing stage where the TI was low-pass filtered at a cutoff frequency of 0.6 Hz to suppress fluctuations due to chest compressions as well as high frequency noise. In a second stage, the preprocessed TI signal, pTI, was analyzed to detect the local maxima and minima. Each local maximum and minimum were characterized by its time of occurrence, $t_{\max_i}$ or $t_{\min_i}$, and amplitude, $Z_{\max_i}$ or $Z_{\min_i}$, respectively as shown in **Figure 6**.

Each detected local maximum was a potential ventilation. To decide whether a maximum corresponded to a ventilation, the inflation amplitude ($A = Z_{\max_i} - Z_{\min_i}$) and inflation time ($d = t_{\max_i} - t_{\min_i}$) were first computed. Then, in the third stage, a decision algorithm decided if a local maximum was a ventilation based on A and d. Three were the requirements for a potential ventilation to be classified as ventilation. The value of d should exceed a minimum static threshold ($d_{\min} = 0.5$ s); the inflation amplitude, A, should be above a dynamic threshold (Th_v) that represents the weighted average of the minimum amplitude of the last 17 ventilations, and finally, the time interval between the actual fluctuation and last detected ventilation should exceed a refractory period ($T_{ref} = 1.4$ s).

This ventilation detector was used to detect the instants of ventilations, and these instants were used to compute the instantaneous ventilation rate, which is reported every 15 s as the ventilation rate provided in the last minute. The global quality metrics of every episode

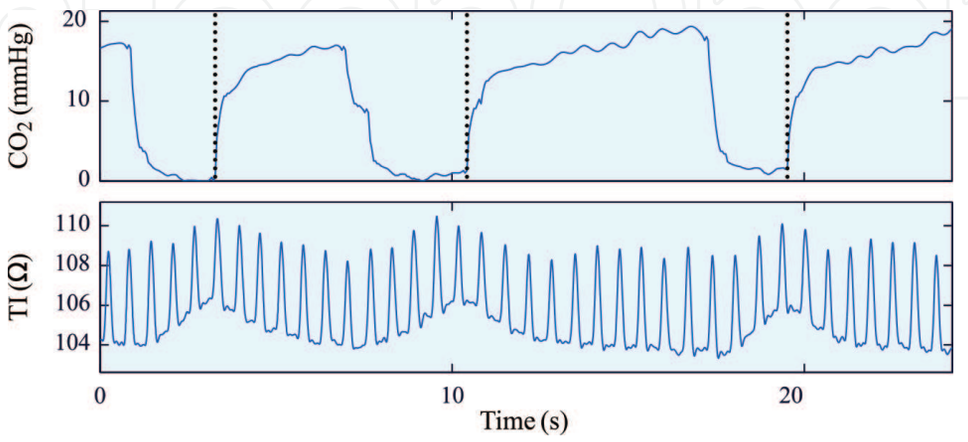

Figure 5. A segment of an episode of the dataset. From top to bottom, the capnogram and the TI. The black dotted lines represent the ventilations annotated in the capnogram.

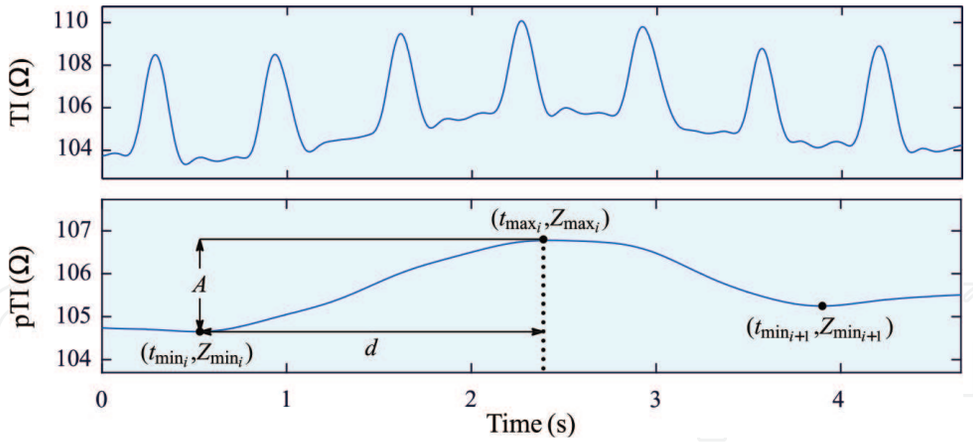

Figure 6. A short segment showing how preprocessing reveals the fluctuation caused by a ventilation. The inflation amplitude, *A*, and inflation time, *d*, are depicted as well as the local maximum and minima.

were also computed, namely the mean ventilation rate and the FMH, the latter to evaluate hyperventilation.

2.2. Evaluation of the ventilation detector

The feasibility and accuracy of the TI signal as a surrogate of the capnogram to measure ventilation metrics was evaluated using the test set. Distributions for each metric obtained from the TI and from the capnogram were analyzed independently applying the one sample Kolmogorov-Smirnov normality test. For normal distributions, the two-sample t-test was performed to test for equal means, and for not normal distributions, the Mann-Whitney U test was used to test for equal medians. The limits of agreement (LOA) between the values obtained from the TI and from the capnogram were analyzed using Bland-Altman plots for each metric.

The ventilation detector showed a median (interquartile range) SE of 92.2% (87.4–95.8), and a median PPV of 81.0% (67.2–90.5). These scores are similar to those reported by other authors as Risdal et al. [35] and Edelson et al. [34]. Nevertheless the proposed method was tested with an independent gold standard, annotated in the capnogram, and it requires a much simpler processing which would permit an easier integration in an AED.

Table 1 is a summary of the ventilation quality metrics computed from the TI and compared to those obtained from the capnogram. Data are presented as mean (standard deviation). The distributions of the FMH obtained from the TI and capnogram were not normal, although they did have equal medians ($p = 0.66$). Mean and instantaneous ventilation rates came from normal distributions. The mean ventilation rate and the FMH obtained from TI and capnogram showed equal means, with mean errors of 1.54 min^{-1} and 1%. That was not the case for the instantaneous ventilation rate, with different mean ($p < 0.001$) and a mean error of 3.30 min^{-1}.

Figure 7 shows the Bland-Altman plots for each ventilation quality metric, and the corresponding 95% LOA depicted with horizontal lines. For the quality metrics, both the mean

Metric	Gold standard	TI	Error	*p*
Mean ventilation rate (min^{-1})	9.54 (2.94)	10.87 (2.68)	1.54 (1.44)	0.07
FMH (%)	11.39 (18.35)	10.09(16.88)	1.29 (2.59)	0.66*
Instantaneous ventilation rate (min^{-1})	10.23 (4.29)	13.09 (4.52)	3.30 (2.88)	<0.001

*The *p*-values obtained from the t-test and Mann–Whitney U test are expressed for each metric.

Table 1. Mean (SD) values computed from the gold standard and from the TI for each ventilation quality metric and the error.

ventilation rate and the FMH showed minor errors, with small LOAs. These results support the use of the TI to accurately evaluate the ventilation metrics when debriefing resuscitation episodes.

The Bland Altman plot for the instantaneous ventilation rate showed large LOAs, in the range of −8 to 5 ventilations per minute. These results question the accuracy of the method based on the TI to monitor the ventilation rate every 15 s.

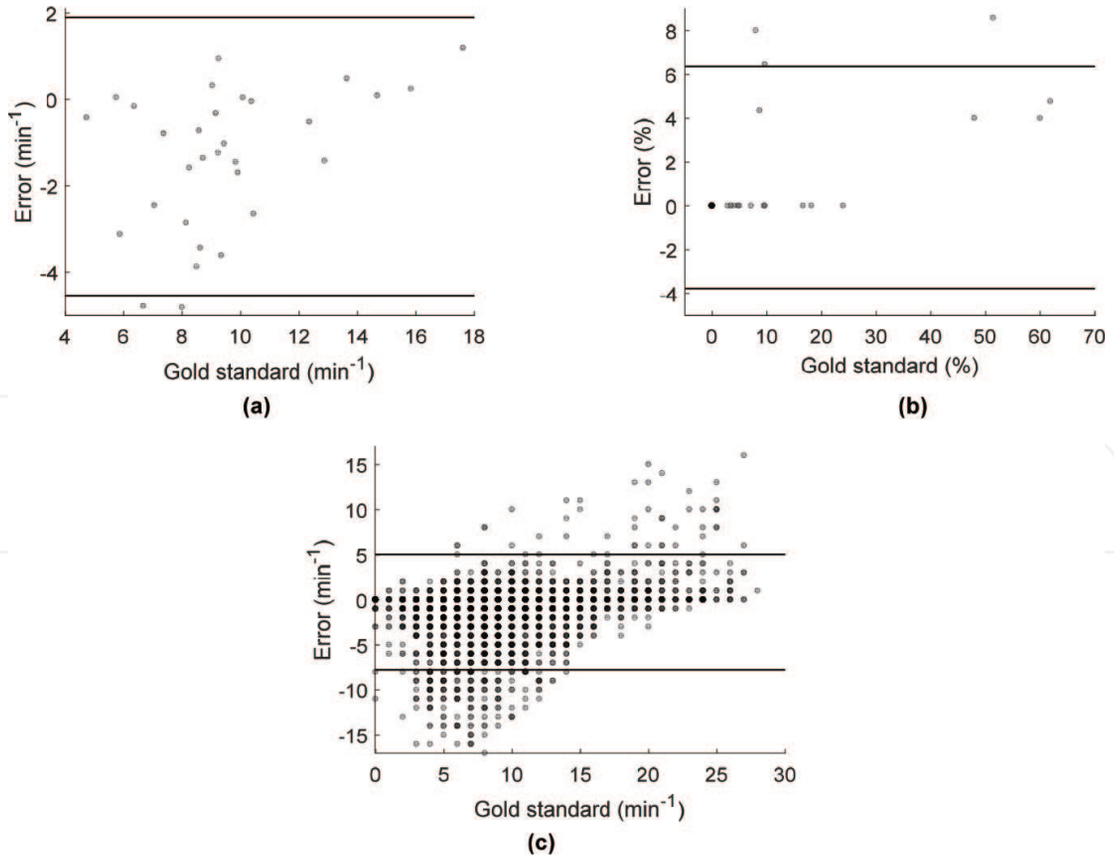

Figure 7. Bland-Altman plots for mean ventilation rate, FMH, and instantaneous ventilation rate are represented in a, b, and c panels respectively. The 95% LOA is depicted in black dashed lines.

3. The use of capnography to monitor ventilation rate

Capnography is a noninvasive monitoring technique that shows the partial pressure of the exhaled CO_2 of the patient over the time [36]. The initial use of the capnography signal (or capnogram) was for anesthesia monitoring, but its use has expanded to other fields such as emergency medicine as it provides information about CO_2 production levels, lung perfusion and alveolar ventilation among others [37]. Current resuscitation guidelines recommend the use of capnography to confirm endotracheal intubation, detect return of spontaneous circulation, monitor the effectiveness of chest compressions and monitor ventilation rate [8].

Advanced monitor/defibrillators used by medical personnel include modules that show the capnogram of the patient during CPR. In current commercial equipment, two main acquisition techniques are used: mainstream and sidestream capnography [38]. The mainstream technology has an infrared light sensor which is placed directly in the main way of expired flow to measure the absorption of CO_2. In sidestream, the expired gases are continuously aspirated from a 1–2 m long sampling tube, and the sensor is placed at the end. **Figure 8** shows the general structure of both acquisition technologies.

The capnogram shows the evolution of the CO_2 expired during the ventilations provided to the patient in cardiac arrest, where the cycle of every ventilation is visible. Four phases are visible in the cycle of each ventilation [39], as illustrated in **Figure 9**: the inspiration baseline (phase I), the expiration upstroke (phase II), the expiratory plateau (phase III) and the expiration down stroke (phase IV). The maximum value observed in the third phase is the so-called $EtCO_2$ (End-tidal CO_2). In hemodynamically stable patients, the value is about 35–45 mmHg, similar to the partial pressure of the CO_2 in the blood [37, 41]. During cardiac arrest, the elimination of CO_2 is reduced and it is accumulated in the tissues. This is because an abrupt

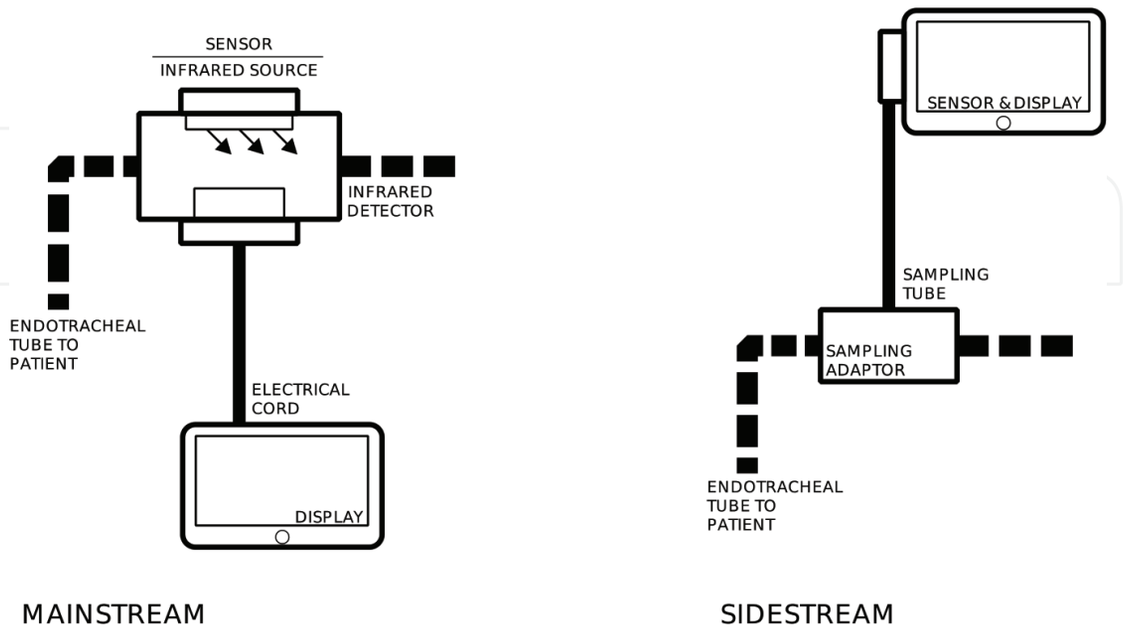

Figure 8. General schemes of mainstream and sidestream technologies to acquire the capnogram.

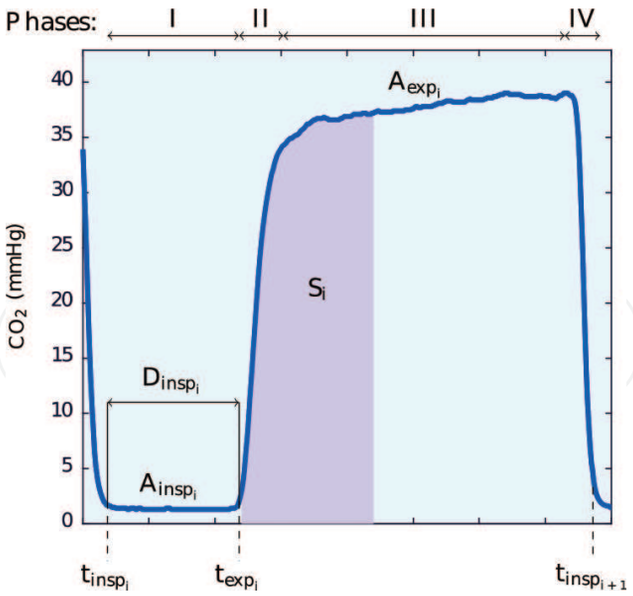

Figure 9. Basic waveform of the capnography signal during a cycle of ventilation. Four phases of the cycle and the features for automatic ventilation detection are shown. Adapted from [40].

decrease in cardiac output implies a reduced CO_2 transportation from the tissues to the lungs, and therefore $EtCO_2$ values decrease almost to zero. Effective chest compressions or recovering pulse make this value increase [42, 43].

During CPR, chest compressions may induce artifacts that corrupt the capnogram. Idris et al. [44] analyzed 210 patients and they detected artifacts in the capnography signal in 154 of 210 episodes, an incidence of 73.3%. More recently, Leturiondo et al. [45] reported an incidence of 42% (99 of 232 episodes showed artifacts). The source and level of the corruption is not well defined yet, and depends on both the patient and the way CPR is performed. Bottom panels of the cases represented in **Figure 10** show examples of the capnogram for four patients, uncorrupted in panels a and c, and corrupted by chest compression artifact in panels b and d. The interference caused by chest compressions complicate the design of automatic ventilation detection algorithms based on the capnogram that would permit the monitoring of ventilation rate and the retrospective debriefing of resuscitation episodes.

The first algorithm to automatically detect ventilations during CPR in the capnogram was proposed by Edelson et al. [34]. They used both the capnogram and the impedance signal to detect the ventilation instants, combining two finite-state-machines. The capnogram-based algorithm provided SE/PPV of 82%/91%. A similar algorithm was proposed by Leturiondo et al. [45] based exclusively on the capnogram with SE/PPV above 95% for uncorrupted intervals, and the accuracy decreased during chest compressions. Both proposals [34, 45] developed the algorithm using as ground truth the ventilations annotated manually in the impedance signal. As it can be observed in **Figure 10** the impedance signal is highly affected by the CPR artifact, and the amplitude of the fluctuations caused by ventilations is not constant, it has been reported to be nonlinear with the tidal volume for all the population [31]. Both factors question the reliability of the ground truth used to evaluate the algorithms.

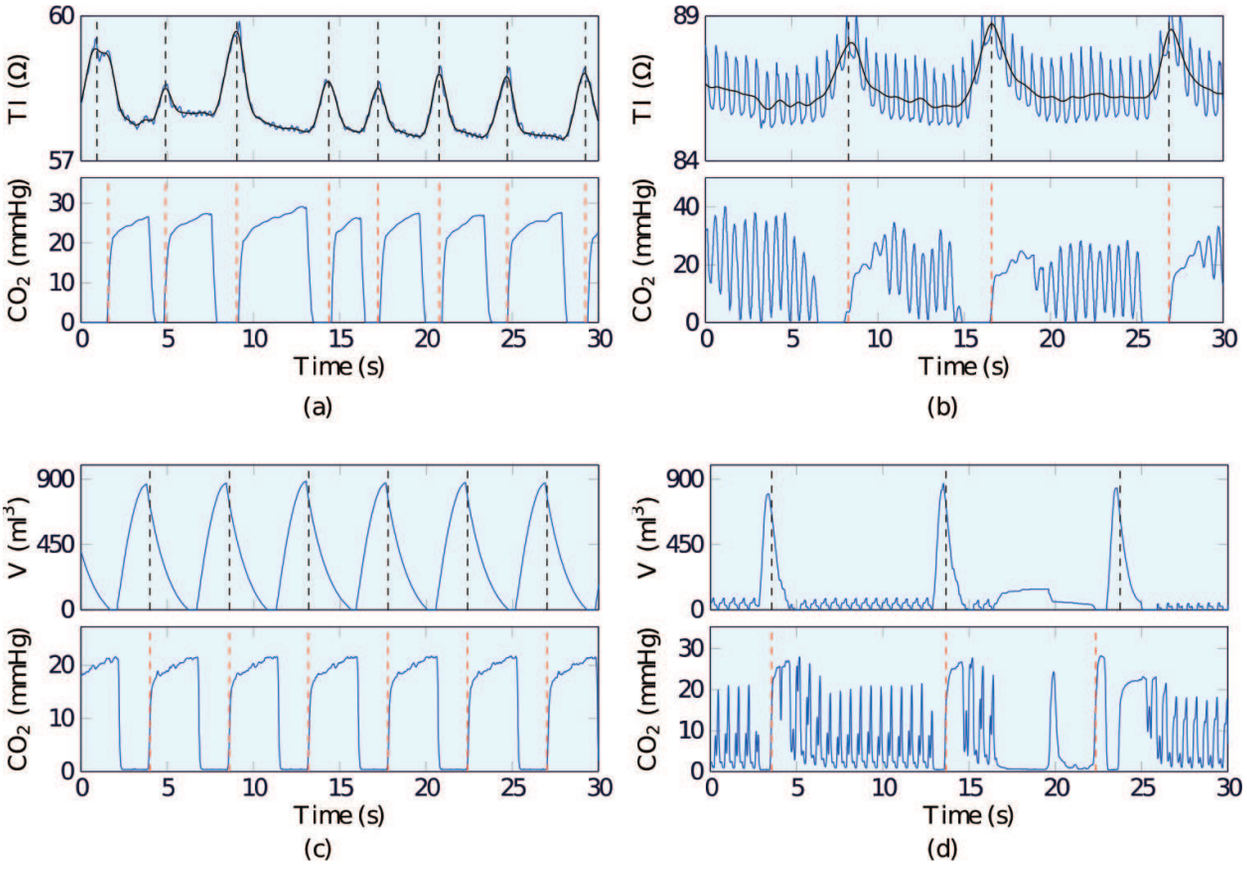

Figure 10. Examples of the capnogram (bottom) and the signal used to annotate the gold standard ventilations (top) are shown for the OHD (panels a and b) and for the IHD (panels c and d). For the OHD, the raw impedance signal (blue) and the filtered impedance signal (black) are shown, and for the IHD the volume signal. In both cases, black vertical lines show the annotated ventilations in the gold standard, and red vertical lines the detected ventilations in the capnogram.

3.1. An automated ventilation detector based on the capnogram

This section describes an algorithm developed using the gas exchange flow measured by a ventilator to annotate the ground truth for the ventilations instants [40]. To the best of our knowledge, this is the only ventilation detector tested with the most reliable ground truth.

Two datasets were used to develop and test the algorithm: an In-Hospital Dataset (IHD) and Out-of-Hospital Dataset (OHD). A total of 83 episodes (62 in-hospital and 21 out-of-hospital) were considered with a duration of 4880 min. The episodes included 16,899 and 29,841 ventilations, with a percentage of 38 and 8% of the time with compressions for the OHD and the IHD, respectively. The general characteristics of both datasets are summarized in **Table 2**. Each episode of the IHD contained the capnogram, and the airflow and air volume signals provided by the ventilator; the instants of the ventilations were annotated based on the volume of the flow signal, as shown in **Figure 10**. Chest compression intervals were identified by medical annotations and abrupt increases in arterial blood pressure. The cases in the OHD included the capnogram, the TI and the CD signals. The CD was used to identify chest compression intervals, while TI and CD were the ground truth to mark ventilations manually. **Figure 10** shows epochs of episodes included in both datasets. For each panel, the top figure shows the independent gold standard (volume signal for IHD and the thoracic impedance signal for OHD), and in the bottom the capnography. The ventilations

Parameter	OHD	IHD
Number of episodes	62	21
Total duration (min)	2545	2335
Total number of ventilations (% with CPR)	16,899 (38)	29,841 (8)
Instantaneous ventilation rate (min^{-1})	9.9 (8.7–13.1)	14.3 (12.6–18.2)
Minutes with hyperventilation per episode (%)	10 (2–35)	14 (0–88)

The instantaneous ventilation rate and minutes with hyperventilation are given per episode as median (interquartile range).

Table 2. Characteristics of both out-of-hospital (OHD) and in-hospital (IHD) datasets.

marked in the gold standard are depicted with black dashed lines. Both gold standards show fluctuations concurrently with the capnography signal for each ventilation. A total of 37 episodes randomly selected from the OHD dataset were used to design and train the algorithm; the test set was conformed with the remaining 25 cases of the OHD and the 21 IHD cases.

The method relies on the computation of the values corresponding to the features shown in **Figure 9**. First, the signal is preprocessed with a low-pass filter with a cutoff frequency of 10 Hz; then values of the waveform below 5 mmHg are set to zero. Potential ventilations are detected between the start of inspiration, t_{insp} (insufflation during ventilation), and the start of expiration, t_{exp} (deflation during ventilation). Both instants are computed based on the positive and negative peaks in the first difference of the signal. Then the following six features, depicted in **Figure 9** are computed:

- Duration of inspiration baseline, D_{insp}.
- Mean value of the signal during plateau, A_{exp}.
- Area of the first second of the expiratory plateau, S_{exp}.
- Relative increase of the signal, computed as:

$$A_r = \frac{A_{\exp} - A_{insp}}{A_{\exp}}, \tag{1}$$

where A_{insp} is the mean amplitude of the signal during inspiration baseline.

- Interval between actual potential ventilation and the last detected ventilation, t_{ref}.

The algorithm discriminates real ventilations based on fixed thresholds for D_{insp} and t_{ref}, and adaptive thresholds for A_{exp}, S_{exp} and A_r. The adaptation for the kth ventilation was computed based on the last p ventilations according to the following equation:

$$Th_k = \frac{w}{p} \sum_{n=k-p}^{k} x_n, \tag{2}$$

where w is a weighting factor between 0 and 1 and x_n represents the value of the feature for ventilation n. A more detailed description of the algorithm can be found in [40]. **Figure 10** shows examples of the algorithm performance. The black dashed lines represent the manual ventilation annotations in the gold standard, and the red dashed lines correspond to the ventilations detected by the algorithm.

As for the TI-based detector, the detected ventilations were used to compute the instantaneous ventilation rate, and the global ventilation metrics per episode.

3.2. Evaluation of the ventilation detector

The algorithm showed overall SE and PPV values above 99% and 97%, respectively. For the OHD, the median (interquartile range) SE and PPV per patient were 99.1 (96.9–99.8)% and 97.0 (95.9–98.9)%. When only the intervals with chest compressions were considered the SE and PPV were 99.0 (95.7–100)% and 97.6(94.8–100)%. For the IHD, SE and PPV were 100 (99.8–100)% and 100 (99.8–100)%. During compressions the performance dropped slightly to 99.8 (98.7–100)% and 98.3 (92.9–100)%, respectively.

The concordance correlation coefficient on ventilation rate measured as proposed in [46] was higher than 0.98 for both datasets, even during chest compressions. **Figure 11** shows the

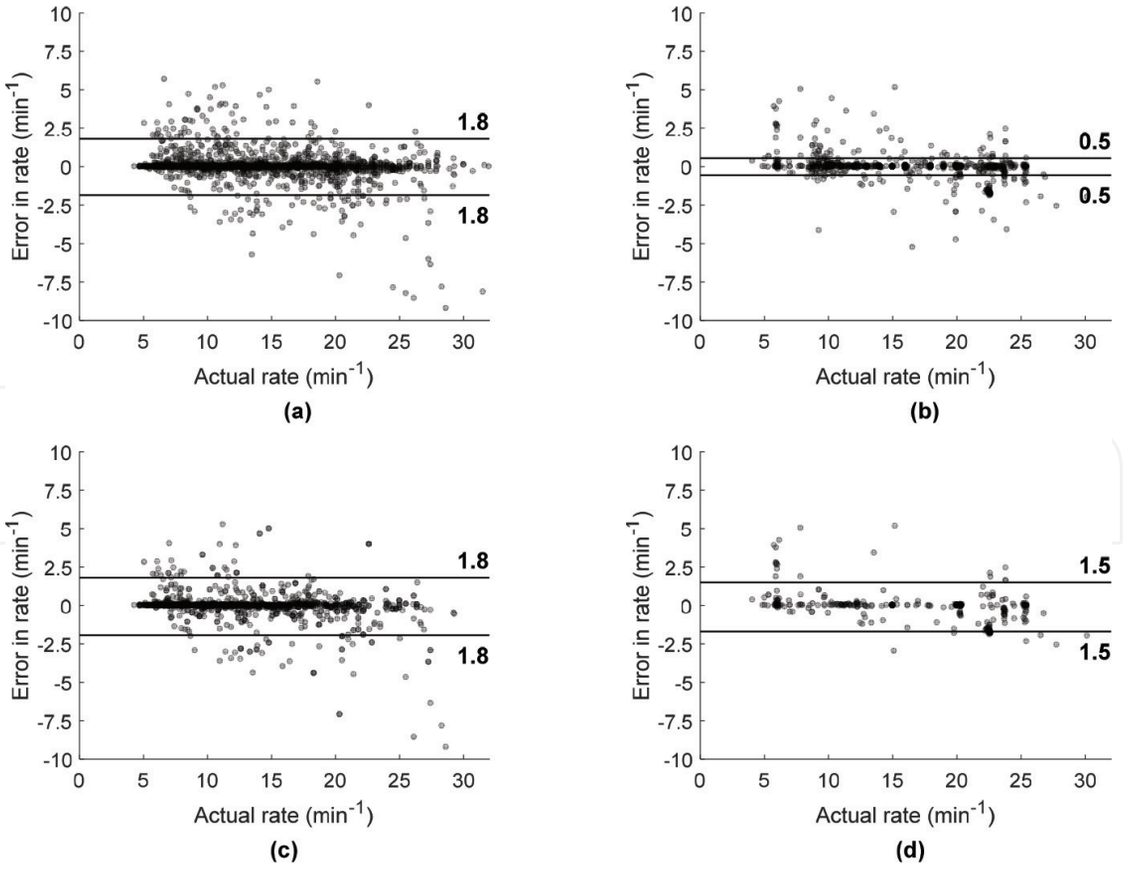

Figure 11. Bland-Altman plots for the instantaneous ventilation rate computed for the OHD (panels a and c) and for the IHD (panels b and d). The limits for the 95% level of agreement are depicted, in 1.82 and 1.8 min^{-1} (during chest compressions) for the OHD, and in 0.55 and 1.50 min^{-1} (during chest compressions) for the IHD.

	Gold standard	Algorithm	*p*
OHD			
Mean ventilation rate (min^{-1})	11.74 (10.34–15.47)	12.11 (10.56–15.37)	0.88
FMH (%)	2.56 (0–34.77)	2.50 (0–34.51)	0.94
Instantaneous ventilation rate (min^{-1})	9.07 (12.44–17.28)	9.23 (12.56–17.31)	0.79
IHD			
Mean ventilation rate (min^{-1})	14.02 (12.53–17.70)	14.02 (12.48–17.77)	1
FMH (%)	5.49 (0–81.08)	5.48 (0–80.39)	1
Instantaneous ventilation rate (min^{-1})	13.98 (12.98–18.98)	13.98 (12.98–18.98)	0.52

All *p* values were calculated using Mann-Whitney U test.

Table 3. Median (interquartile range) values computed from the gold standard and from the capnogram for each ventilation quality metric.

Bland-Altman plots and the 95% LOA between the gold standard and the algorithm, which was lower than 1.85 in any case. These results show that this capnogram-based method reliably estimates the instantaneous rate.

The detailed results for the ventilation quality metrics are shown in **Table 3**. It can be observed that the mean ventilation rate and the FMH showed equal distributions ($p > 0.05$) when compared to the ground truth for both the OHD and IHD episodes. The unsigned errors were close to zero for both metrics and for both datasets. These results support the use of this method to retrospectively debrief resuscitation episodes.

4. Discussion and conclusions

In this chapter, the monitoring of ventilations provided during out-of-hospital CPR was addressed with two objectives. First, giving feedback on the instantaneous ventilation rate to rescuers. Second, to allow retrospectively evaluation of ventilation rates and hyperventilation metrics during resuscitation episodes.

The analysis focused on the feasibility of the TI acquired by the defibrillation pads, and the capnogram to accurately report feedback on ventilation. Methods based exclusively on each of the signals were proposed and statistically evaluated. These methods could be integrated in commercial defibrillation equipment, the TI-based algorithm in any AED or monitor/defibrillators, and the capnogram-based algorithm in any equipment that includes capnography.

Several aspects deserved attention in the development of the algorithms. In the setting of the procedure, the gold standard was carefully selected. In the case of the TI, manual annotations were defined in the capnogram, as a result of the consensus of three experts. In the case of the capnogram, the independent signal used as gold standard was the gas volume exchanged measured by an external ventilator. In both cases, the gold standard was

annotated using an independent signal, including the gas exchange information, which is, in our opinion, the most reliable signal. This is a key factor when evaluating the accuracy and reliability of the methods.

In any case, the simplicity of the method was a priority. The algorithms proposed do not rely on complicated or computationally intensive signal processing techniques, so they could be integrated in current defibrillation equipment without much increase of computational requirements.

The scores obtained for the TI-based method are similar to those previously reported in terms of SE (around 90%), and slightly below for PPV. For the capnogram-based method, SE/PPV was both above 97% in any dataset, even when chest compressions were provided.

Both methods are valid to be integrated in the software provided to retrospectively review the quality of the ventilations. Errors below 2 min^{-1} in the mean rate and about 1% in the FMH for both the TI and the capnogram are sufficient for an accurate retrospective evaluation. The integration of these methods in the revision software provided by commercial equipment would permit debriefing on ventilation after cardiac arrest. The American Heart Association emphasizes the post-even analysis of the data, which contributes to the continuous quality improvement, closing the gap between the ideal and the actual performance of OHCA resuscitation. Excessive ventilation rates are often observed during CPR both out- and in-hospital cardiac arrest [14], and code team debriefing with audiovisual feedback has been associated with a decrease in mean ventilation rates from 18 to 13 min^{-1} [34, 47].

For the audiovisual feedback to the rescuer, the instantaneous rate should be provided to the rescuers, associated, if necessary with hyperventilation alarms. The instantaneous rate, as computed in the methods proposed, would permit feedback every 15 s, which is a reasonable compromise to follow the feedback and adhere to the recommendations of the guidelines. The method proposed on the capnogram was very reliable with errors below 2 min^{-1} for any dataset even during chest compressions. That was not the case for the TI, as the mean error for the instantaneous rate was above 3 min^{-1}. Two are the reasons that make difficult the automated detection of ventilations in the TI. First, the fluctuations caused by ventilations are very variable, even for the same patient, so adaptive thresholding is required for the algorithm. Panel a in **Figure 10** shows clear examples in which similar ventilation cycles in the capnogram appear with very different amplitudes in the impedance waveform. Therefore, it is very difficult to define a universally valid TI amplitude threshold for the detection of ventilations. Second, artifacts caused by chest compressions and other noise make difficult to automatically detect every ventilation.

Finally, it should be stated that the results and conclusions presented in this chapter are limited by the specific characteristics of the data used. Using the TI or the capnogram from other equipment, with different electronic circuitry and defibrillation pads, may require readapting the values and thresholds of the algorithms and may result in different values of the performance metrics.

Acknowledgements

This work has been partially supported by the Spanish Ministerio de Economía y Competividad, jointly with the Fondo Europeo de Desarrollo Regional (FEDER), project TEC2015-64678-R, by the University of the Basque Country via project EHU16/18, the Ayudas a Grupos de Investigación GIU17/031 and the unit UFI11/16, and by the Basque Government through the grant PRE_2017_1_0112.

Author details

Andoni Elola, Erik Alonso, Elisabete Aramendi* and Unai Irusta

*Address all correspondence to: elisabete.aramendi@ehu.es

University of the Basque Country, Bilbao, Spain

References

[1] Zheng Z-J, Croft JB, Giles WH, Mensah GA. Sudden cardiac death in the United States, 1989 to 1998. Circulation. 2001;**104**(18):2158-2163

[2] Atwood C, Eisenberg MS, Herlitz J, Rea TD. Incidence of EMS-treated out-of-hospital cardiac arrest in Europe. Resuscitation. 2005;**67**(1):75-80

[3] Bayés de Luna A, Coumel P, Leclercq JF. Ambulatory sudden cardiac death: Mechanisms of production of fatal arrhythmia on the basis of data from 157 cases. American Heart Journal. 1989;**117**(1):151-159

[4] Cobb LA, Fahrenbruch CE, Olsufka M, Copass MK. Changing incidence of out-of-hospital ventricular fibrillation, 1980-2000. Journal of the American Medical Association. 2002;**288**(23):3008-3013

[5] Chugh SS, Jui J, Gunson K, Stecker EC, John BT, Thompson B, et al. Current burden of sudden cardiac death: Multiple source surveillance versus retrospective death certificate-based review in a large U.S. community. Journal of the American College of Cardiology. 2004;**44**(6):1268-1275

[6] Rea TD, Eisenberg MS, Sinibaldi G, White RD. Incidence of EMS-treated out-of-hospital cardiac arrest in the United States. Resuscitation. 2004;**63**(1):17-24

[7] Larsen MP, Eisenberg MS, Cummins RO, Hallstrom AP. Predicting survival from out-of-hospital cardiac arrest: A graphic model. Annals of Emergency Medicine. 1993;**22**(11):1652-1658

[8] Soar J, Nolan JP, Böttiger BW, Perkins GD, Lott C, Carli P, et al. European resuscitation council guidelines for resuscitation 2015: Section 3. Adult advanced life support. Resuscitation. 2015;**95**:100-147

[9] Koster RW, Baubin MA, Bossaert LL, Caballero A, Cassan P, Castrén M, et al. European resuscitation council guidelines for resuscitation 2010 section 2. Adult basic life support and use of automated external defibrillators. Resuscitation. 2010;**81**(10):1277-1292

[10] Bag-Mask Ventilation Fails to Improve on Endotracheal Intubation in Cardiac Arre [Internet]. [cited 2018 Jan 29]. Available from: https://www.escardio.org/The-ESC/Press-Office/Press-releases/bag-mask-ventilation-fails-to-improve-on-endotracheal-intubation-in-cardiac-arrest

[11] Berg RA, Hemphill R, Abella BS, Aufderheide TP, Cave DM, Hazinski MF, et al. Part 5: Adult basic life support: 2010 American Heart Association Guidelines for Cardiopulmonary Resuscitation and Emergency Cardiovascular Care. Circulation. 2010;**122**(18 Suppl 3):S685-S705

[12] Abella BS, Alvarado JP, Myklebust H, Edelson DP, Barry A, O'Hearn N, et al. Quality of cardiopulmonary resuscitation during in-hospital cardiac arrest. Journal of the American Medical Association. 2005;**293**(3):305-310

[13] McInnes AD, Sutton RM, Orioles A, Nishisaki A, Niles D, Abella BS, et al. The first quantitative report of ventilation rate during in-hospital resuscitation of older children and adolescents. Resuscitation. 2011;**82**(8):1025-1029

[14] Aufderheide TP, Sigurdsson G, Pirrallo RG, Yannopoulos D, McKnite S, von Briesen C, et al. Hyperventilation-induced hypotension during cardiopulmonary resuscitation. Circulation. 2004;**109**(16):1960-1965

[15] O'Neill JF, Deakin CD. Do we hyperventilate cardiac arrest patients? Resuscitation. 2007;**73**(1):82-85

[16] Milander MM, Hiscok PS, Sanders AB, Kern KB, Berg RA, Ewy GA. Chest compression and ventilation rates during cardiopulmonary resuscitation: The effects of audible tone guidance. Academic Emergency Medicine: Official Journal of the Society for Academic Emergency Medicine. 1995;**2**(8):708-713

[17] Woodson RD. Physiological significance of oxygen dissociation curve shifts. Critical Care Medicine. 1979;**7**(9):368-373

[18] Madden JA. The effect of carbon dioxide on cerebral arteries. Pharmacology & Therapeutics. 1993;**59**(2):229-250

[19] Karlsson T, Stjernström EL, Stjernström H, Norlén K, Wiklund L. Central and regional blood flow during hyperventilation. An experimental study in the pig. Acta Anaesthesiologica Scandinavica. 1994;**38**(2):180-186

[20] Yannopoulos D, McKnite S, Aufderheide TP, Sigurdsson G, Pirrallo RG, Benditt D, et al. Effects of incomplete chest wall decompression during cardiopulmonary resuscitation on coronary and cerebral perfusion pressures in a porcine model of cardiac arrest. Resuscitation. 2005;**64**(3):363-372

[21] Kramer-Johansen J, Edelson DP, Losert H, Köhler K, Abella BS. Uniform reporting of measured quality of cardiopulmonary resuscitation (CPR). Resuscitation. 2007;**74**(3):406-417

[22] Kerber RE, Grayzel J, Hoyt R, Marcus M, Kennedy J. Transthoracic resistance in human defibrillation. Influence of body weight, chest size, serial shocks, paddle size and paddle contact pressure. Circulation. 1981;**63**(3):676-682

[23] Gruben KG. Mechanics of pressure generation during cardiopulmonary resuscitation [thesis]. 1994

[24] Fitzgibbon E, Berger R, Tsitlik J, Halperin HR. Determination of the noise source in the electrocardiogram during cardiopulmonary resuscitation. Critical Care Medicine. 2002;**30**(4):S148-S153

[25] Stecher FS, Olsen J-A, Stickney RE, Wik L. Transthoracic impedance used to evaluate performance of cardiopulmonary resuscitation during out of hospital cardiac arrest. Resuscitation. 2008;**79**(3):432-437

[26] Losert H, Risdal M, Sterz F, Nysaether J, Köhler K, Eftestøl T, et al. Thoracic impedance changes measured via defibrillator pads can monitor ventilation in critically ill patients and during cardiopulmonary resuscitation. Critical Care Medicine. 2006;**34**(9):2399-2405

[27] Pellis T, Bisera J, Tang W, Weil MH. Expanding automatic external defibrillators to include automated detection of cardiac, respiratory, and cardiorespiratory arrest. Critical Care Medicine. 2002;**30**(4):S176-S178

[28] Alonso E, Aramendi E, Daya M, Irusta U, Chicote B, Russell JK, et al. Circulation detection using the electrocardiogram and the thoracic impedance acquired by defibrillation pads. Resuscitation. 2016;**99**:56-62

[29] Alonso E, Ruiz J, Aramendi E, González-Otero D, de Gauna SR, Ayala U, et al. Reliability and accuracy of the thoracic impedance signal for measuring cardiopulmonary resuscitation quality metrics. Resuscitation. 2015;**88**:28-34

[30] Hull E, Irie T, Heemstra H, Wildevuur CR. Transthoracic electrical impedance: Artifacts associated with electrode movement. Resuscitation. 1978;**6**(2):115-124

[31] Roberts K, Srinivasan V, Niles DE, Eilevstjønn J, Tyler L, Boyle L, et al. Does change in thoracic impedance measured via defibrillator electrode pads accurately detect ventilation breaths in children? Resuscitation. 2010;**81**(11):1544-1549

[32] Risdal M, Aase SO, Kramer-Johansen J, Eftesøl T. Automatic identification of return of spontaneous circulation during cardiopulmonary resuscitation. IEEE Transactions on Biomedical Engineering. 2008;**55**(1):60-68

[33] Husoy J, Eilevstjønn J, Eftestøl T, Aase SO, Myklebust H, Steen PA. Removal of cardiopulmonary resuscitation artifacts from human ECG using an efficient matching pursuit-like algorithm. IEEE Transactions on Biomedical Engineering. 2002;**49**(11):1287-1298

[34] Edelson DP, Eilevstjønn J, Weidman EK, Retzer E, Hoek TLV, Abella BS. Capnography and chest-wall impedance algorithms for ventilation detection during cardiopulmonary resuscitation. Resuscitation. 2010;**81**(3):317-322

[35] Risdal M, Aase SO, Stavland M, Eftestøl T. Impedance-based ventilation detection during cardiopulmonary resuscitation. IEEE Transactions on Biomedical Engineering. 2007;**54**(12):2237-2245

[36] Terndrup TE, Rhee J. Available ventilation monitoring methods during pre-hospital cardiopulmonary resuscitation. Resuscitation. 2006;**71**(1):10-18

[37] Sanders AB. Capnometry in emergency medicine. Annals of Emergency Medicine. 1989;**18**(12):1287-1290

[38] Jaffe MB. Mainstream or sidestream capnography? Environment. 2002;**4**:5

[39] Pantazopoulos C, Xanthos T, Pantazopoulos I, Papalois A, Kouskouni E, Iacovidou N. A review of carbon dioxide monitoring during adult cardiopulmonary resuscitation. Heart, Lung & Circulation. 2015;**24**(11):1053-1061

[40] Aramendi E, Elola A, Alonso E, Irusta U, Daya M, Russell JK, et al. Feasibility of the capnogram to monitor ventilation rate during cardiopulmonary resuscitation. Resuscitation. 2017;**110**:162-168

[41] Trilĺo G, von Planta M, Kette F. ETCO2 monitoring during low flow states: Clinical aims and limits. Resuscitation. 1994;**27**(1):1-8

[42] Sheak KR, Wiebe DJ, Leary M, Babaeizadeh S, Yuen TC, Zive D, et al. Quantitative relationship between end-tidal carbon dioxide and CPR quality during both in-hospital and out-of-hospital cardiac arrest. Resuscitation. 2015;**89**:149-154

[43] Pokorná M, Nečas E, Kratochvíl J, Skřipskỳ R, Andrlík M, Franěk O. A sudden increase in partial pressure end-tidal carbon dioxide (PETCO2) at the moment of return of spontaneous circulation. The Journal of Emergency Medicine. 2010;**38**(5):614-621

[44] Idris AH, Daya M, Owens P, O'Neill S, Helfenbein ED, Babaeizadeh S, et al. Abstract 83: High incidence of chest compression oscillations associated with capnography during out-of-hospital cardiopulmonary resuscitation. Circulation. 2010;**122**(21 Supplement):A83

[45] Leturiondo M, de Gauna SR, Ruiz JM, Gutiérrez JJ, Leturiondo LA, González-Otero DM, et al. Influence of chest compression artefact on capnogram-based ventilation detection during out-of-hospital cardiopulmonary resuscitation. Resuscitation. 2018;**124**:63-68

[46] Lin LI. A concordance correlation coefficient to evaluate reproducibility. Biometrics. 1989;**45**(1):255-268

[47] Morrison LJ, Neumar RW, Zimmerman JL, Link MS, Newby LK, McMullan PW, et al. Strategies for improving survival after in-hospital cardiac arrest in the United States: 2013 consensus recommendations: A consensus statement from the American Heart Association. Circulation. 2013;**127**(14):1538-1563